A Pole Detection and Geospatial Localization Framework using LiDAR-GNSS Data Fusion

Durga Prasad Bavirisetti*†, Gabriel Hanssen Kiss*, Frank Lindseth*
*Department of Computer Science, Norwegian University of Science and Technology, Trondheim, Norway
Email: durga.bavirisetti@ntnu.no, gabriel.kiss@ntnu.no, frankl@ntnu.no
†Department of Mobility, SINTEF AS, Trondheim, Norway
Email: durga.bavirisetti@sintef.no

***Abstract*—The integration of Light Detection and Ranging (LiDAR) and Global Navigation Satellite System (GNSS) technologies marks a significant advancement in the fields of autonomous driving and intelligent transportation systems. This research introduces a methodology for geolocalizing road objects, specifically poles, by leveraging the detailed spatial data from LiDAR combined with the location capabilities of GNSS, while carefully accounting for these sensor offsets. Our approach takes advantage of the synergy between LiDAR's exceptional spatial resolution and GNSS's global positioning capability. This precision is crucial for the navigation systems of autonomous vehicles. By processing LiDAR data to detect objects and calculate their positions relative to the sensor, and then transforming these positions into global coordinates using inverse geodesic calculations, we present a methodology that can perform object geolocation in various environments. This paper details the development of the methodology, the challenges encountered, and the solutions devised, showcasing the approach's performance through experimental results and suggests future directions for further research.**

***Index Terms*—autonomous vehicles, LiDAR, GNSS, sensor fusion, geolocalization, offset compensation**

I. Introduction

The rapid advancement and deployment of autonomous vehicles necessitate highly accurate geolocalization systems capable of precisely identifying and positioning road objects [1]. Traditional navigation systems, predominantly reliant on Global Navigation Satellite System (GNSS) data, offer valuable global positioning information but often lack the spatial resolution required for detailed environmental mapping [2]. Conversely, Light Detection and Ranging (LiDAR) technology provides high-resolution spatial data but lacks global context [3]. This research presents a fusion methodology that integrates the detailed spatial data from LiDAR with the global positioning capabilities of GNSS, incorporating sensor offset compensation for road object geolocalization. This approach addresses a critical challenge in autonomous navigation by ensuring mapping of detected objects to global coordinates, thereby enhancing the operational safety and efficiency of autonomous vehicles within dynamic environments.

II. Literature Review

The fusion of LiDAR and GNSS data for object localization has been a focal point of research in the realm of autonomous navigation and intelligent transportation systems [4]. LiDAR sensors are lauded for their high spatial resolution and precision in mapping the surrounding environment, providing detailed 3D point clouds [5]. Conversely, GNSS offers invaluable global positioning information, albeit with limitations in spatial resolution and susceptibility to signal obstructions in urban settings [6].

The concept of sensor fusion, particularly integrating LiDAR with GNSS and Inertial Navigation Systems (INS), has been explored extensively to overcome the individual limitations of these sensors [7]. The integration aims to leverage the high-resolution spatial data of LiDAR and the global positioning capabilities of GNSS, providing a comprehensive solution for object localization. Sensor offset, the physical displacement between the LiDAR sensor and the GNSS receiver, poses a significant challenge in mapping detected objects to global coordinates. Previous studies have highlighted the importance of compensating for these offsets to improve localization accuracy [8].

Recent advancements in deep learning have further propelled the field, enabling more sophisticated object detection algorithms capable of processing complex LiDAR data [9]. These developments underscore the potential of combining LiDAR's detailed environmental scans with GNSS's global positioning to achieve precise object localization, a critical aspect of autonomous vehicle navigation.

III. Methodology

The proposed method is presented in Figure 1. It outlines the process for real-time pole detection and geospatial localization using LiDAR and GNSS data. It begins with data acquisition and processing of LiDAR and GNSS data, followed by pole detection using signal images. Next, it identifies the nearest point to the detected pole in range images and determines the nearest 3D point on the pole. The vehicle's heading is computed, allowing for the transformation of LiDAR coordinates to the sensor frame. This leads to the calculation of distance, azimuth, elevation and, absolute azimuth for each detected pole. An offset from the sensor to GNSS coordinates is calculated, followed by an inverse geodesic calculation to geolocalize the pole. The final output is the mapping of geolocalized poles.

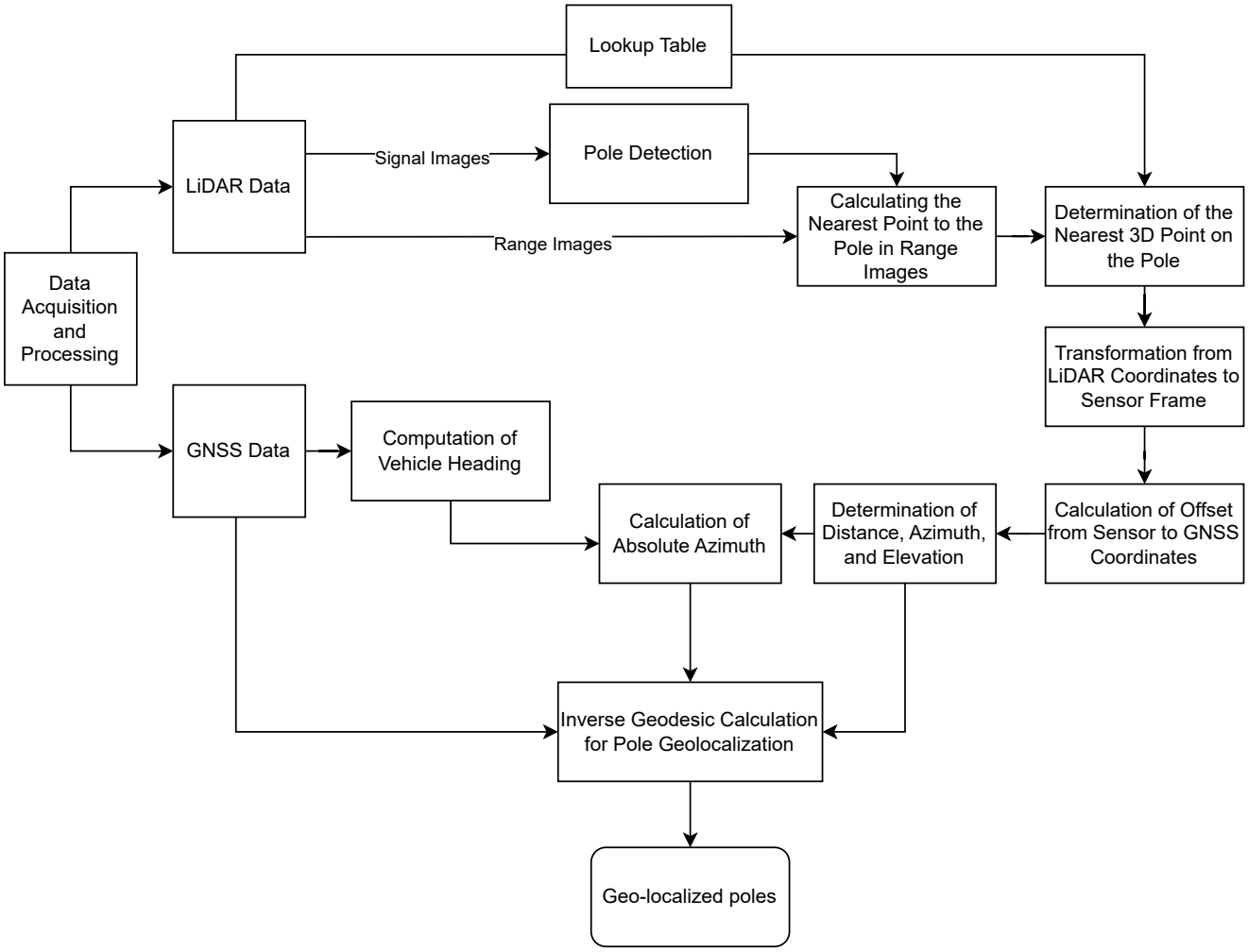

Fig. 1: Block Diagram for Geolocalization Process

A. Data Acquisition and Processing

Data were acquired from an autonomous vehicle equipped with an OS1-128 LiDAR sensor and a GNSS device, capturing comprehensive spatial and global positioning data. The LiDAR sensor, characterized by its high resolution and wide field of view, provides detailed 3D point clouds of the surrounding environment, while the GNSS device offers global positioning coordinates essential for mapping the detected objects to a global context. Details on the vehicle setup are provided in section IV.

B. Signal and Range Image Analysis for Pole Detection

Signal and range image analysis for pole detection involves converting the 3D point cloud data from a LiDAR sensor into 2D images that represent the intensity (signal image) and distance (range image) of each point from the sensor. This conversion facilitates the application of image processing and object detection algorithms. For pole detection, algorithms analyze these images to identify patterns and features characteristic of poles, such as verticality, continuity, and distinctiveness from the background, based on their signal strength and spatial location within the range image. Advanced machine learning models, particularly convolutional neural networks (CNNs), can be trained on labeled datasets to recognize and accurately detect poles in these images.

C. Pole Detection Framed as an Object Detection Problem

Our primary objective is to develop a pipeline for the geolocalization of poles. To tackle this, we've framed it as an object detection challenge. Accordingly, we've selected YOLOv5-a simple, lightweight, and efficient Convolutional Neural Network (CNN) designed for object detection tasks [10]. It is known for its rapid processing speed (achieving over 100 FPS with GPU support) and high accuracy, making it a preferred choice for 2D perception tasks. Additionally, employing recent advancements in object detection could further enhance detection performance for this purpose. In this work, we trained YOLOV5 model to detect poles and used the

pre-trained model to detect poles within the signal images. For each detected pole, extracted the bounding box and used it to isolate the portion of the LiDAR range image corresponding to the pole.

D. Calculating the Nearest Point to the Pole in Range Images

To calculate the nearest point to the pole in range images, the process involves analyzing depth data to identify the shortest distance between the sensor and the detected object within the pole's identified region. Mathematically, for each pixel i in the pole's region within the range image, with a distance value d_i, the goal is to find $d_{\text{min}} = \min(d_i)$ where i ranges over all pixels that belong to the pole. This operation pinpoints the closest part of the pole to the LiDAR sensor, enabling localization.

E. Determination of the Nearest 3D Point on the Pole

The determination of the nearest 3D point on a pole from LiDAR data involves analyzing spatial coordinates to locate the point closest to the sensor. Given the pixel coordinates (x, y) in the range image and depth d where the pole is detected, the 3D coordinates (X, Y, Z) can be computed[1]. This process utilizes the LiDAR's intrinsic parameters and a transformation matrix mapping 2D image coordinates to 3D world coordinates, often incorporating trigonometric calculations based on the sensor's field of view and the angular position of the pixel.

F. Transformation from LiDAR Coordinates to Sensor Frame

The transformation from LiDAR coordinates to the sensor frame is an essential process in sensor fusion and spatial data analysis, aiming to align LiDAR-detected points with the sensor or vehicle coordinate system. This alignment is crucial for integrating LiDAR data with data from other sensors, which is vital for accurate positioning and navigation.

LiDAR systems measure environmental data as a point cloud in a coordinate system centered on the LiDAR device, with each point representing a coordinate (x, y, z) based on the distance measured from the LiDAR's position. However, to utilize LiDAR data in conjunction with other sensor data effectively, it is necessary to transform these points to the sensor frame, often based on the vehicle's orientation, a robotic platform, or any system integrating multiple sensor types.

The transformation process involves both rotation and translation to align the LiDAR points with the orientation and position of the sensor frame. This can be encapsulated into a transformation matrix that relocates the points accurately within the sensor frame when applied to the LiDAR frame points.

The transformation from the LiDAR coordinate frame to the sensor frame for the Ouster LiDAR[2] can be represented by a homogeneous transformation matrix $M_{\text{lidar}\to\text{sensor}}$, combining a rotation matrix R and a translation vector T into a single 4×4 matrix:

$$M_{\text{lidar}\to\text{sensor}} = \begin{pmatrix} -1 & 0 & 0 & 0 \\ 0 & -1 & 0 & 0 \\ 0 & 0 & 1 & \Delta z \\ 0 & 0 & 0 & 1 \end{pmatrix} \tag{1}$$

In this matrix:

- The rotation part involves flipping the x and y axes, necessary due to the differing orientations of the LiDAR and sensor coordinate systems.
- The translation part includes a shift along the z-axis by Δz, the difference in height between the LiDAR's mounting point and the origin of the sensor frame, here Δz is 0.038195 meters or 3.8195 centimeters.

Given a point $(x, y, z, 1)$ in the LiDAR frame, its coordinates $(x', y', z', 1)$ in the sensor frame can be obtained by:

$$\begin{pmatrix} x' \\ y' \\ z' \\ 1 \end{pmatrix} = M_{\text{lidar}\to\text{sensor}} \cdot \begin{pmatrix} x \\ y \\ z \\ 1 \end{pmatrix} \tag{2}$$

This operation will rotate and translate the LiDAR point to the sensor coordinate system, aligning it with data from other sensors and the vehicle's reference frame. This transformation is essential for applications requiring navigation, mapping, and autonomous decision-making.

G. Calculation of Offset from Sensor to GNSS Coordinates

For accurately positioning LiDAR-detected objects relative to a vehicle's GNSS device, calculating the offset between the LiDAR sensor and the GNSS coordinates is essential. This calculation involves two primary steps. Firstly, the GNSS device and LiDAR sensor offsets relative to a vehicle's reference point are defined as $\mathbf{O}_{\text{GNSS}}$ and $\mathbf{O}_{\text{LIDAR}}$, respectively. Secondly, the offset from the LiDAR sensor to the GNSS device, denoted as$\Delta\mathbf{O}$, is calculated by subtracting $\mathbf{O}_{\text{GNSS}}$ from $\mathbf{O}_{\text{LIDAR}}$:

$$\Delta\mathbf{O} = \mathbf{O}_{\text{LiDAR}} - \mathbf{O}_{\text{GNSS}} \tag{3}$$

Finally, this offset is applied to the coordinates of an object detected by LiDAR, $\mathbf{P}_{\text{LiDAR}}$, to transform them into the GNSS coordinate system:

$$\mathbf{P}_{\text{GNSS}} = \mathbf{P}_{\text{LiDAR}} + \Delta\mathbf{O} \tag{4}$$

H. Determination of Distance, Azimuth, and Elevation

The determination of azimuth, elevation, and distance from an observation point to an object in three-dimensional space is crucial for a wide range of applications, including navigation and remote sensing. For a point with coordinates (x, y, z) in a Cartesian coordinate system, the following calculations are performed:

1) **Distance Calculation**: The distance, D, between the observation point and the object is fundamental for establishing their spatial relationship. It is calculated using the three-dimensional extension of the Pythagorean theorem:

$$D = \sqrt{x^2 + y^2 + z^2} \tag{5}$$

[1]https://static.ouster.dev/sdk-docs/reference/lidar-scan.html

[2]https://static.ouster.dev/sensor-docs/image_route1/image_route2/sensor_data/sensor-data.html#lidar-range-data-to-sensor-xyz-coordinate-frame

2) **Azimuth Calculation**: The azimuth, θ, is the horizontal angle from a reference direction (typically true north) to the projection of the point onto the xy-plane. It is calculated as follows:

$$\theta = \arctan 2(y, x) \times \frac{180}{\pi} \tag{6}$$

3) **Elevation Calculation**: The elevation, ϕ, indicates the vertical angle from the horizontal plane to the object. It is given by:

$$\phi = \arcsin\left(\frac{z}{D}\right) \times \frac{180}{\pi} \tag{7}$$

These mathematical procedures allow for the localization and tracking of objects, thereby enhancing navigation systems, astronomical studies, and surveillance technologies.

I. Computation of Vehicle Heading

The computation of vehicle heading involves determining the direction in which a vehicle is moving, typically expressed in degrees from a reference direction (usually true north). This is calculated using the difference in geographic coordinates (latitude and longitude) between two points along the vehicle's path [11][3]. Mathematically, if (ϕ_1, λ_1) and (ϕ_2, λ_2) represent the latitude and longitude of two successive positions, the heading θ can be calculated using:

$$\Delta\lambda = \lambda_2 - \lambda_1, \tag{8}$$

$$X = \sin(\Delta\lambda) \cdot \cos(\phi_2), \tag{9}$$

$$Y = \cos(\phi_1) \cdot \sin(\phi_2) - \sin(\phi_1) \cdot \cos(\phi_2) \cdot \cos(\Delta\lambda), \tag{10}$$

$$\theta = \text{atan2}(X, Y). \tag{11}$$

where $\Delta\lambda = \lambda_2 - \lambda_1$, and the result of `atan2` gives the heading in radians, which can be converted to degrees. This formula accounts for the spherical nature of the Earth when calculating the heading. This method offers a way to derive the heading based on latitude and longitude changes, crucial for navigation and tracking movement when the vehicle is in moving state.

J. Calculation of Absolute Azimuth

The calculation of absolute azimuth incorporates an observer's or vehicle's heading into the determination of an object's true direction relative to geographic north [12][4]. This adjustment is vital for navigation, ensuring that azimuth readings are correctly aligned with global coordinates.

Given a relative azimuth, θ, defined as the angle between the observer's forward direction and the line of sight to an object, and the vehicle's heading, H, the absolute azimuth, Θ_{abs}, can be calculated using the equation:

$$\Theta_{\text{abs}} = (\theta + H) \mod 360 \tag{12}$$

This equation adjusts the relative azimuth by adding the vehicle's heading to it, then applying a modulus of 360 degrees to ensure the azimuth value falls within the standard range of 0 to 360 degrees. This method enables the direction finding and positioning in relation to the Earth's cardinal directions.

K. Inverse Geodesic Calculation for Pole Geolocalization

The inverse geodesic calculation for pole geolocalization utilizes the WGS84 geodesic model [13] to transform relative movements into absolute geographic coordinates[5]. This method employs an initial latitude and longitude, alongside an azimuth (bearing from North) and a distance to a target, to compute the target's final geographic position. This calculation is vital for projecting the location of objects, such as poles detected by sensors, relative to their surroundings on the Earth's surface.

Utilizing the `Geodesic.Direct` method from the Geodesic library, the calculation is as follows:

Given an initial point (lat, lon), azimuth α, and distance d, the final point's coordinates $(\text{lat}_2, \text{lon}_2)$ are determined by:

$$\text{Geodesic.Direct}(\text{lat}, \text{lon}, \alpha, d) \rightarrow (\text{lat}_2, \text{lon}_2) \tag{13}$$

This methodology is crucial for mapping detected objects' positions onto global positioning systems, thereby enhancing navigation and tracking applications.

(a) Front and Rear View of the Vehicle

(b) Top View of the Vehicle with Sensor Locations

Fig. 2: NAPLab Research Platform

IV. Experiments and Results

Our experimental setup integrates a comprehensive methodology for geolocalizing road objects, particularly poles, using a fusion of LiDAR and GNSS data, accompanied by sensor offset compensation.

A. Vehicle Setup

The data collection for this research was conducted using the NAPLab research platform of NTNU[6], as shown in Figure 2a, which is a fully electric Kia e-Niro. This vehicle is outfitted with NVIDIA DRIVE software and an extensive sensor array for comprehensive data gathering. The sensor setup includes eight cameras: three facing forward inside the vehicle, two mounted on each mirror for both forward and backward side views, and an additional rear-facing camera. Additionally, the vehicle is equipped with three LiDAR units: a 360-degree,

[3]https://www.movable-type.co.uk/scripts/latlong.html
[4]https://geographiclib.sourceforge.io/html/python/
[5]https://geographiclib.sourceforge.io/html/python/code.html
[6]https://www.ntnu.edu/idi/naplab/vehicles

128-channel unit on the top, a 180-degree, 16-channel unit at the front, and a nearly 270-degree unit aimed at the rear right side. The vehicle also has two radars, with one facing forward at the front and the other facing backward at the rear, alongside a highly accurate GNSS system for positioning data.

In the current study, data were collected using the top view LiDAR (Ouster 128 Channel) and the left GNSS of the vehicle. The approximate locations of the sensors on the vehicles are depicted in Figure 2b. These measurements span from the center of the back wheel to various devices, all formatted according to the Nvidia coordinate system guidelines. For detailed information on the Nvidia coordinate system, refer to the Nvidia DriveWorks documentation[7]. For the GNSS devices, while the x and z coordinates remain constant for both devices, the y coordinates vary, indicating their placement on either side of the vehicle (left with a negative y-value, right with a positive y-value). Specifically, the GNSS devices are positioned at $x = -0.32\,m$, $y = \pm 0.51\,m$, and $z = 1.24\,m$ and the top LiDAR situated at $x = 0.7\,m$, $y = 0.0\,m$, $z = 1.8\,m$. Thus, the offset $\Delta\mathbf{O}$ in Equation 3 is determined to be $x = -1.02\,m$, $y = 0.51\,m$, and $z = 0.56\,m$, through the computation of the difference between the positions of the left GNSS device and the LiDAR sensor. These meticulous measurements are critical for understanding the spatial relationships between the various sensors mounted on the vehicle, ensuring accurate data collection and interpretation in our research.

B. Data acquisition and LiDAR Image Processing

As the part of our project, the E39 Hemnekjølen was chosen as the test location. As shown in Figure 3a, its comprehensive 4.2 km route is ideal for setting up and surveying snowplow stakes. This route goes through many different areas, including mountains, open spaces, and forest. It has various types of safety barriers and changing road signs. The presence of a large parking area at the route's western end offers convenient opportunities for turnaround, enhancing the logistical efficiency of our experiments. The selection of Hjemnekjølen as the test location is pivotal, as it involved the manual measurement of the GNSS locations for poles installed on both sides of the road. Figure 3a depicts these meticulously measured pole locations at Hjemnekjølen. To facilitate our experiments, lidar data and GNSS tracks were captured from a vehicle operating within this locale.

In Figure 3b, we present a visualization of the data acquired from the GNSS, illustrating the vehicle's trajectory and the spatial distribution of measured pole locations. The vehicle's GNSS track is depicted as a bold blue line, representing the sequential positions recorded by the satellite navigation system as the vehicle navigated the area. This track offers insight into the vehicle's movements across a diverse landscape, as captured in the two-dimensional plane of latitude and longitude. Superimposed upon this trajectory are the measured locations of poles, marked by green crosses. These fixed positions serve

[7]https://docs.nvidia.com/drive/driveworks-3.5/dwx_coordinate_systems.html

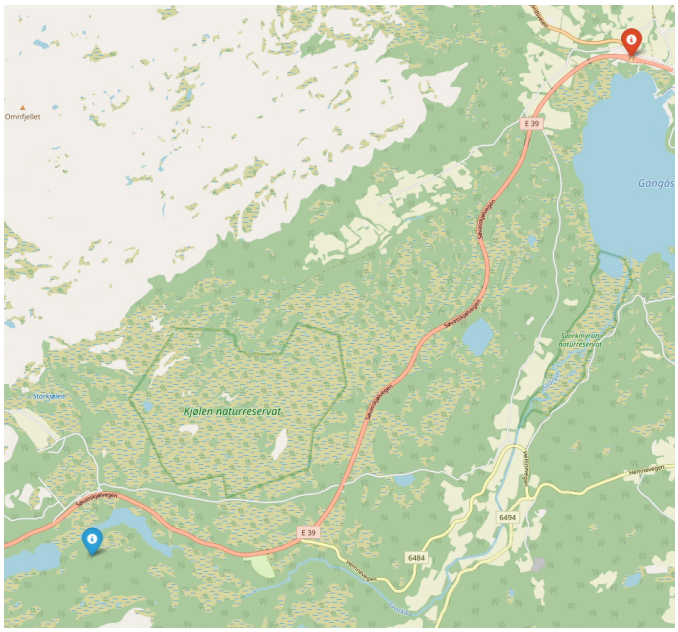

(a) Route of the Vehicle

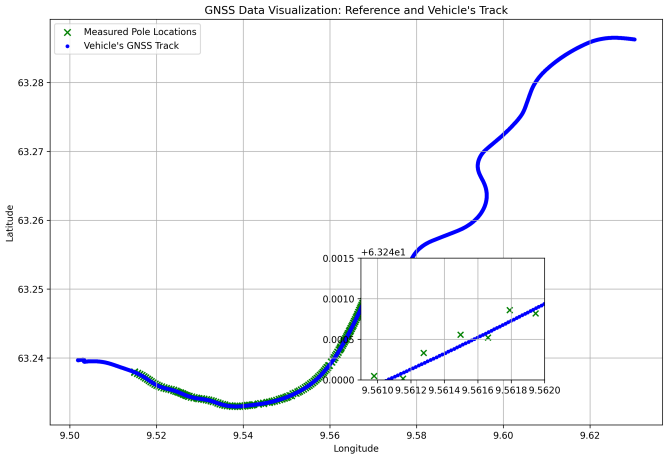

(b) Measured Pole Locations with Left GNSS Track

Fig. 3: Experimental Setup at E39 Hemnekjølen: (a) Route of the Vehicle, (b) Measured Pole Locations along with Vehicle's Left GNSS Track

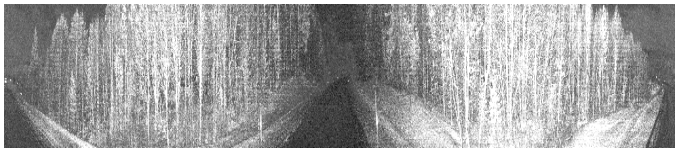

(a) LiDAR Signal Image

(b) LiDAR Range Image

Fig. 4: Sample 360-degree LiDAR Signal and Range Images

as reference points within the data set, against which the GNSS-derived path of the vehicle can be analyzed for accuracy and precision. A closer examination is provided by the inset within the figure, which zooms into a more narrowly defined segment of the route. Here, we can observe the fine-scale relationship between the vehicle's path and the poles with enhanced clarity. The inset's zoom level, indicated by the scale factor `"+6.324e1"`, allows for a detailed analysis of the GNSS track in relation to the fixed objects, aiding in the assessment of the system's locational accuracy.

Figures 4a and 4b showcase sample LiDAR signal and range images, providing a 360-degree view from the test location. These images were captured using the Ouster LiDAR, which is mounted on top of the vehicle as depicted in Figure 2[8].

C. Pole Detection

We extracted LiDAR signal images from the data gathered at our test location, and then we designed a dataset specifically for pole detection, aimed at training the YOLOv5 model. It comprises a training set with 753 images, making up the majority of the data to aid in comprehensive learning of features and patterns. The validation set includes 125 images, which is used to evaluate the model's performance on data it hasn't been trained on, ensuring the model can accurately generalize to new situations. Notably, there is no separate test set in this configuration, with the focus being on training and validation phases. Preprocessing includes resizing images to 1024x128 and applying a series of augmentations like shear, grayscale conversion, and adjustments in hue, saturation, brightness, and exposure to bolster the model's generalization capabilities. These augmentations, along with targeted modifications to the bounding boxes such as rotation, shear, and noise adjustments, are designed to increase the dataset's diversity and realism. This approach optimizes the YOLOv5 model's training process, enhancing its efficiency in detecting poles.

The trained model showcases a architecture with 213 layers and over 7 million parameters, operating at an efficiency of 15.8 GFLOPs. It achieved a high precision of 0.903 and a recall of 0.848, indicating its effectiveness in accurately detecting and correctly identifying poles from the images. The model's mean Average Precision (mAP) at an Intersection over Union (IoU) threshold of 0.5 is notably high at 0.872, reflecting its strong capability in making precise predictions.

After successfully training the model, we applied the pre-trained model to data collected at the test location, contained in ROS bags. These bags include both LiDAR images and GNSS information, facilitating the real-time geolocation of poles. Figures 5a and 5b showcase a labeled LiDAR image from the dataset and the poles predicted on test images, respectively. Both training and testing images were obtained from the ROS bag file.

D. Geolocalization of the poles

We have explored the process of capturing real-time data from a vehicle outfitted with advanced sensing technology.

[8]https://ouster.com/insights/blog/the-camera-is-in-the-lidar

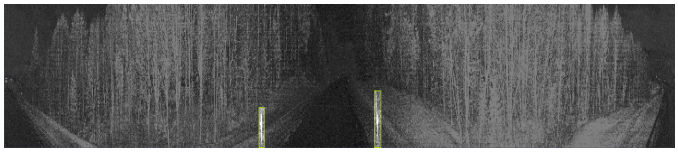

(a) Labeled LiDAR Image from the Dataset

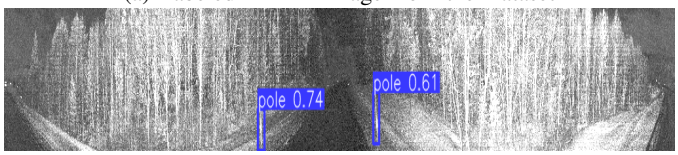

(b) Test Image with Predictions from the ROS Bag File

Fig. 5: Labeled LiDAR Image from the Dataset Alongside a Test Image with Predictions

This setup includes a high-precision LiDAR sensor for detailed environmental mapping and a GNSS system for accurate positioning. The procedure starts with collecting LiDAR and GNSS data, which leads to the creation of signal and range images from the LiDAR scans. These images are subsequently analyzed to identify poles.

Critical to this methodology is the calculation of their nearest points within range images (Section III-D) and computing the 3D coordinates using the range data and Ouster lookup table (Section III-E. Furthermore, along with the transformation from LiDAR coordinates to the sensor frame (Section III-F), to improve the geolocalization accuracy, we also calculate the offset from sensor to GNSS coordinates (Section III-G), taking into account the physical placement differences between the LiDAR sensor and the GNSS device on the vehicle.

Subsequently, we calculated the distance, azimuth, and elevation of objects relative to the sensor, as outlined in Section III-H. Additionally, the heading of the vehicle, which is essential for determining the vehicle's direction based on GNSS data, was computed as detailed in Section III-I. This process is pivotal for the calculation of the absolute azimuth of detected objects, as discussed in Section III-J.

The final step in this process, detailed in Section III-K, involves using inverse geodesic calculations. These calculations are based on the WGS84 geodetic model, allowing for the accurate projection of localized poles onto the global coordinate system. This technique ensures a detailed mapping of road objects onto a global scale. Figure 6 presents a signal image showcasing the distance and geolocation information for these predcited pole objects.

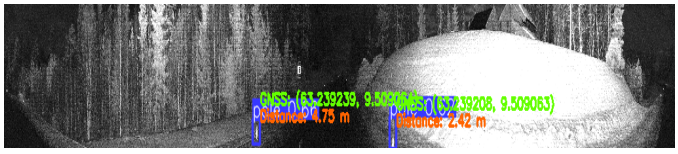

Fig. 6: Signal Image Showcasing the Distance and Geolocation Information for the Predicted Poles

E. Transforming and Filtering GNSS Data for Spatial Analysis

This section outlines a method for visualizing GNSS (Global Navigation Satellite System) data to examine the spatial relationships among manually measured pole locations, vehicle GNSS data, and the geolocations of poles predicted by our method. We start by converting the reference GNSS data, originally in the Universal Transverse Mercator Zone 33 (UTM33) coordinate system, into the World Geodetic System 1984 (WGS84) format for latitude and longitude, using the pyproj library[9]. This step ensures that our geolocation data aligns with global standards for accuracy and interoperability. Next, we filter the GNSS data for objects and vehicles according to the geographical limits defined by the reference pole data. Since the vehicle's travel path is broader than the area covered by the reference data, this filtering process focuses our analysis on the relevant area, discarding data points outside our region of interest.

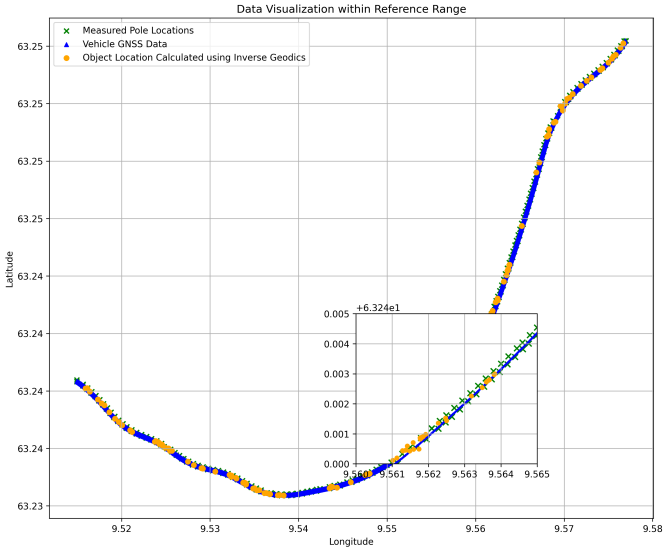

Fig. 7: Comprehensive Representation of the Spatial Distribution of Reference GNSS Data, and the Filtered Vehicle and Object GNSS Data Within Predefined Geographical Boundaries, Differentiated by Distinct Color-Coded Markers

The Figure 7 illustrates the geospatial distribution of GNSS data within a specified reference range. It presents a scatter plot where the x-axis represents longitude and the y-axis represents latitude. Three distinct sets of data are visualized: Measured Pole Locations is marked with green 'x' symbols, Vehicle GNSS Data is indicated by blue triangles, and Object Location Calculated using Inverse Geodics is denoted by orange circles. An inset in the lower left portion of the graph provides a zoomed-in view of a particular section of this trajectory, offering a more granified look at the spatial relationship among the data in this region. The blue and orange markers closely align along the path indicated by the green 'x' markers, demonstrating the performance of the pole localization of the proposed method in relation to the reference data. This visual alignment suggests a precision in geolocalization, which is critical for the navigational systems of autonomous vehicles. The grid within the inset enhances the readability and allows for better estimation of the specific positioning differences among the data.

V. Discussion

This section delves into the merits and limitations of the proposed method for pole detection and geospatial localization, employing a fusion of LiDAR and GNSS data complemented by sensor offset compensation. Our analysis encompasses various facets of the methodology, highlighting its significance in autonomous vehicle navigation and intelligent transportation systems.

A. Advantages

The proposed methodology introduces several notable advantages that significantly contribute to its application in autonomous driving and intelligent transportation systems. Firstly, the integration of LiDAR's spatial resolution with GNSS's locational accuracy[10] offers precision in object geolocalization, particularly for road poles in our case. This fusion addresses the critical need for exact object positioning, crucial for navigation and safety in autonomous vehicles.

Moreover, the method's approach to sensor offset compensation enhances the accuracy of mapping detected objects to global coordinates. This meticulous adjustment for sensor displacement exemplifies the detailed consideration of spatial relationships in sensor fusion technologies. Furthermore, the versatility of the approach across varied environments underscores its robustness, making it a viable solution for diverse geographical settings.

Additionally, the practicality and reliability of the proposed methodology are validated through experimental results. These findings not only demonstrate the method's effectiveness but also its applicability in real-world scenarios, reinforcing its potential for widespread adoption in the field.

B. Drawbacks and Challenges

Despite its advantages, the proposed method is not without its drawbacks and challenges. The complexity of the data fusion process, coupled with sensor offset compensation, presents potential limitations, especially in real-time applications.

The success of the methodology heavily relies on the quality of both LiDAR and GNSS data. Inconsistencies or inaccuracies in this data can significantly affect localization precision. Moreover, the calibration of sensors to account for offsets necessitates meticulous attention to detail, with any discrepancies potentially leading to errors in object positioning.

The efficacy of our proposed system is largely contingent on the object detection algorithm's efficiency. For illustrative purposes, we selected a detection threshold of 0.7 in Figure 7. This setting resulted in the non-detection of certain poles and,

[9]https://pyproj4.github.io/pyproj/stable/

[10]https://www.kartverket.no/en/on-land/posisjon/guide-to-cpos

despite the high threshold, some instances of misidentification were still evident. Another critical component of our approach involves pinpointing the 3D coordinates on a pole to facilitate the geolocalization of objects. In our study, we assumed the closest point on the pole to the vehicle to be this critical point. Nevertheless, this assumption may not hold if the generated bounding box is disproportionately large, or if another object situated in front of the pole is encompassed within the bounding box. One potential resolution to these challenges is the adoption of more advanced object detection algorithms, such as a state-of-the-art model beyond YOLOV5, or reframing the pole detection task as an instance segmentation problem. Such strategies could mitigate prediction inconsistencies and yield more precise pole locations.

Vehicle heading is another vital factor in the geolocalization process. We have computed the vehicle heading using consecutive GNSS points, which proves effective at higher speeds. However, this method may not be reliable when the vehicle is stationary. To circumvent this limitation, integrating additional sensor data, including extra GNSS units, IMU, and vehicle odometry, may be advantageous. Moreover, employing advanced methods or LiDAR-specific techniques for calculating angles might enhance the accuracy of azimuth, elevation measurements, and ultimately, the determination of the poles' global positions.

C. Future Directions

Addressing the identified challenges offers promising avenues for future research. Optimizing the computational efficiency of the method could enhance its suitability for real-time applications, broadening its applicability in autonomous vehicles. Exploring advanced calibration techniques and improving the robustness of the system against data quality issues are essential steps towards refining the methodology.

Expanding the scope of the method to encompass a wider array of objects and environments could also yield significant benefits. Such advancements would not only augment the versatility of the approach but also contribute to its scalability, making it a more comprehensive solution for autonomous vehicle navigation and intelligent transportation systems.

VI. Conclusion

In our study, we developed a new technique that combines LiDAR and GNSS technology to identify the location of objects like poles on roads, a crucial advancement for autonomous driving and smart transportation systems. By merging detailed LiDAR imagery with GNSS location data, our method enhances the ability of self-driving cars to navigate safely by ensuring the exact placement of road objects is known. Although the method is effective when the vehicle is moving quickly, it faces challenges at slower speeds or when stationary. These challenges stem from reliance on high-quality LiDAR and GNSS data and the need for precise sensor calibration. To address these issues, we suggest incorporating more sensors or adopting different techniques for better direction estimation. Looking forward, optimizing this method for real-time application and extending its use to a wider variety of objects and environments could further benefit autonomous vehicles and intelligent transport systems. Our research presents a new approach to integrating LiDAR and GNSS for object localization, offering significant implications for the future of autonomous navigation.

Acknowledgment

The authors would like to extend their sincere gratitude to the Norwegian Research Council for their generous support of this study. This research was conducted as part of the project titled "Machine Sensible Infrastructure under Nordic Conditions" under the of Project Number 333875.

References

[1] T. Ort, L. Paull, and D. Rus, "Autonomous vehicle navigation in rural environments without detailed prior maps," in *2018 IEEE international conference on robotics and automation (ICRA)*. IEEE, 2018, pp. 2040–2047.

[2] A. M. Hasan, K. Samsudin, A. R. Ramli, R. Azmir, and S. Ismaeel, "A review of navigation systems (integration and algorithms)," *Australian journal of basic and applied sciences*, vol. 3, no. 2, pp. 943–959, 2009.

[3] J. Kocić, N. Jovičić, and V. Drndarević, "Sensors and sensor fusion in autonomous vehicles," in *2018 26th Telecommunications Forum (TELFOR)*. IEEE, 2018, pp. 420–425.

[4] Q. Li, J. P. Queralta, T. N. Gia, Z. Zou, and T. Westerlund, "Multi-sensor fusion for navigation and mapping in autonomous vehicles: Accurate localization in urban environments," *Unmanned Systems*, vol. 8, no. 03, pp. 229–237, 2020.

[5] B. S. Shin and C. K. Toth, "Roadway feature extraction using lidar and gps data," *Photogrammetric Engineering & Remote Sensing*, vol. 74, no. 5, pp. 605–616, 2008.

[6] E. D. Kaplan and C. J. Hegarty, *Understanding GPS: Principles and Applications*. Artech House, 2005.

[7] I. Skog and P. Handel, "In-car positioning and navigation technologies—a survey," *IEEE Transactions on Intelligent Transportation Systems*, vol. 10, no. 1, pp. 4–21, 2009.

[8] Y. Lu, H. Ma, E. Smart, and H. Yu, "Real-time performance-focused localization techniques for autonomous vehicle: A review," *IEEE Transactions on Intelligent Transportation Systems*, vol. 23, no. 7, pp. 6082–6100, 2021.

[9] J. Fayyad, M. A. Jaradat, D. Gruyer, and H. Najjaran, "Deep learning sensor fusion for autonomous vehicle perception and localization: A review," *Sensors*, vol. 20, no. 15, p. 4220, 2020.

[10] G. Jocher, A. Chaurasia, A. Stoken, J. Borovec, Y. Kwon, K. Michael, J. Fang, C. Wong, Z. Yifu, D. Montes *et al.*, "ultralytics/yolov5: v6. 2-yolov5 classification models, apple m1, reproducibility, clearml and deci. ai integrations," *Zenodo*, 2022.

[11] B. Luzum, "Navigation principles of positioning and guidance," 2004.

[12] W. Lowrie and A. Fichtner, *Fundamentals of geophysics*. Cambridge university press, 2020.

[13] C. F. Karney, "Algorithms for geodesics," *Journal of Geodesy*, vol. 87, pp. 43–55, 2013.